The 1st International Workshop on
Bayesian Approach in Civil Engineering (IWOBA 2025)
Hong Kong, China, January 10-12, 2025
Edited by Y.-Q. Ni, Y. Huang, B. Li and H.-W. Li

RELIABILITY-CONSTRAINED BAYESIAN OPTIMIZATION FOR STRUCTURAL DESIGN UNDER UNCERTAINTY

James Whiteley [a] and Jurgen Becque [a]

[a] Department of Engineering, University of Cambridge, JJ Thomson Avenue 7a, Cambridge, UK
E-mails: jw2293@cam.ac.uk, jurgen.becque@eng.cam.ac.uk

Keywords
Reliability-based optimization;
Bayesian optimization;
Prestressed concrete;
Gaussian process;

Abstract

Structural design under uncertainty requires an approach that balances safety, cost, and performance, while accounting for the variability inherent in the design parameters on which real-world engineering problems depend. Traditional deterministic design methods often fall short in such contexts and can lead to overly conservative designs. This paper introduces a reliability-constrained Bayesian optimization framework tailored for structural design problems, where reliability constraints are enforced through probabilistic models. This method's implementation leverages fast, parallel batch optimization with gradient-based techniques, efficiently handling uncertainties drawn from any probability distribution. We apply the proposed method to an analytic test function from the literature, as well as to the design of a prestressed concrete structure. Results indicate the efficiency of our approach in achieving optimized designs that satisfy reliability requirements with reduced computational costs compared to traditional methods from reliability engineering.

1 INTRODUCTION

The design of structures is undertaken under uncertainty. Uncertainty exists in material properties, environmental conditions, structural geometry, loading scenarios and associated with the models used for structural analysis. Modern building codes such as Eurocodes [1] deal with uncertainties in design by adopting a load and resistance factor approach, first introduced by Ellingwood [2] in the early 1980s. Such codes, while comprehensive, cannot account for all possible scenarios inherent in real-world applications. As a result, traditional deterministic design approaches can fail to capture the full extent of design situations.

In contrast to deterministic optimization, which assumes fixed values for parameters, Reliability-based optimization accounts for variability in inputs; probabilistic or chance constraints are used to ensure the design achieves a desired level of reliability. Reliability-based optimization problems are difficult to solve for two main reasons. They are generally non-convex, even if the underlying functions in the constraint and objective are convex, and hence it cannot be guaranteed that a solution is the global optimum [3]. In addition, checking the feasibility of objectives and constraints is computationally expensive because it requires multivariate integration, which is an NP-Hard problem [4]. Classical methods used to solve Reliability-based optimization within the discipline of engineering have been worked on extensively since the 1960s [5]. These methods typically rely on deterministic approximations to evaluate system reliability, and struggle to model complex, highly nonlinear systems. Whilst simulation-based approaches alleviate this issue, they can be prohibitively expensive where computationally demanding numerical models define the optimization objective or constraints. To address these challenges, Bayesian optimization has emerged as a powerful tool for optimizing complex systems under uncertainty with minimal computational cost.

In this paper, we focus on reliability-constrained Bayesian optimization, an extension of standard Bayesian optimization that incorporates objectives and constraints expressed probabilistically. In this framework, engineers can explore optimal trade-offs between performance, safety, and cost, while accounting for uncertainties in the input parameters. We base our work upon recent advances in reliability-constrained Bayesian optimization for structural design, while implementing an approach that leverages fast, parallel batch optimization with gradient-based methods. In addition to a methodology, we present a case study illustrating its application to a real-world prestressed concrete design example.

The paper is organized as follows: Section 2 outlines the proposed surrogate modelling and optimization framework; Section 3 describes our implementation,

which uses automatic differentiation to enable efficient gradient-based optimization; Section 4 shows the results of the method applied to both an analytic test function from the literature, and an engineering example; Section 5 concludes the paper.

2 BAYESIAN OPTIMIZATION WITH CHANCE CONSTRAINTS

This paper considers the following chance-constrained optimization problem:

$$\max_{\boldsymbol{x}\in\mathbb{R}^{\mathrm{d}}} \mathrm{E}[f(\boldsymbol{x},\boldsymbol{\xi})] \quad \mathrm{P}[g_i(\boldsymbol{x},\boldsymbol{\xi})\le 0]\ge 1-\varepsilon_i,\quad \forall\, i=1,\dots,m \qquad (1)$$

where $\boldsymbol{x}\in\mathbb{R}^{\mathrm{d}}$ are deterministic design variables, and $\boldsymbol{\xi}\in\Xi$ are uncertain parameters, drawn from a probability distribution over the domain Ξ. E and P denote an expected value and a probability, respectively. The optimization objective and constraint functions depend on the uncertain parameters, but, in contrast to the design variables, they are not controlled by the optimization procedure. The chance constraints, assumed statistically independent, must hold with a probability of at least $1-\varepsilon$.

Bayesian optimization (BayesOpt) is an approach to global optimization which involves two steps performed sequentially: 1) a surrogate model, based on observed data $D=\{((\boldsymbol{x}_i,\boldsymbol{\xi}_i),f(\boldsymbol{x}_i,\boldsymbol{\xi}_i))\}_{i=1}^{n}$, is created, providing a predictive distribution over unseen points; 2) heuristics (called acquisition functions) based on that predictive distribution are used to choose where to next sample additional data for the surrogate model. The acquisition function itself may be multimodal and hence hard to optimize, and so BayesOpt makes sense primarily in the case where the original functions being modelled are expensive or time-consuming. A tutorial on BayesOpt is given by [6].

2.1 Gaussian process[1]

The canonical surrogate model used in BayesOpt is a Gaussian process, which is briefly described here. A Gaussian process is a collection of random variables, any finite subset of which have a joint Gaussian distribution [7]. A Gaussian process is fully specified by a mean function and covariance function, i.e., $f(\boldsymbol{x})\sim\mathcal{GP}\big(m(\boldsymbol{x}),k(\boldsymbol{x},\boldsymbol{x}')\big)$. Typically, the mean function is set to zero, i.e., $m(\boldsymbol{x})=0$, since the input data can be standardized. The covariance function encodes the belief that points $\boldsymbol{x}_i$, $\boldsymbol{x}_j$ that are close in the input space will have similar function values. The squared exponential covariance function is most common and used in this work:

$$k(\boldsymbol{x},\boldsymbol{x}')=\sigma_f^2\exp\left(-\frac{|\boldsymbol{x}-\boldsymbol{x}'|^2}{2\ell^2}\right) \qquad (2)$$

which has hyperparameters $\boldsymbol{\theta}=(\sigma_f^2,\ell)$, obtained by maximizing the log marginal likelihood $\log p(\boldsymbol{y}\mid\boldsymbol{X},\boldsymbol{\theta})$. Given a set of observations $\boldsymbol{y}=[y_1,\cdots,y_n]\in\mathbb{R}^{\mathrm{n}}$ associated with training inputs $\boldsymbol{X}=[\boldsymbol{x}_1,\cdots,\boldsymbol{x}_n]\in\mathbb{R}^{\mathrm{n\,x\,d}}$ and a set of query points $\boldsymbol{X}^*=[\boldsymbol{x}_1^*,\cdots,\boldsymbol{x}_k^*]\in\mathbb{R}^{\mathrm{k\,x\,d}}$, Gaussian process regression provides a posterior predictive distribution $\boldsymbol{y}^*\mid\boldsymbol{X}^*,\boldsymbol{X},\boldsymbol{y}\sim N(\boldsymbol{\mu}^*,\boldsymbol{\Sigma}^*)$ of the form:

$$\boldsymbol{\mu}^*=\boldsymbol{K}(\boldsymbol{X}^*,\boldsymbol{X})\boldsymbol{K}(\boldsymbol{X},\boldsymbol{X})^{-1}\boldsymbol{y} \qquad (3)$$

$$\boldsymbol{\Sigma}^*=\boldsymbol{K}(\boldsymbol{X}^*,\boldsymbol{X}^*)-\boldsymbol{K}(\boldsymbol{X}^*,\boldsymbol{X})\boldsymbol{K}(\boldsymbol{X},\boldsymbol{X})^{-1}\boldsymbol{K}(\boldsymbol{X},\boldsymbol{X}^*) \qquad (4)$$

where $\boldsymbol{K}(\boldsymbol{X},\boldsymbol{X})\in\mathbb{R}^{\mathrm{n\,x\,n}}$ is the covariance matrix at the previously seen points $K_{ij}=k(\boldsymbol{x}_i,\boldsymbol{x}_j)$, $\boldsymbol{K}(\boldsymbol{X}^*,\boldsymbol{X}^*)\in\mathbb{R}^{\mathrm{k\,x\,k}}$ is the covariance matrix at the query points $K_{ij}=k(\boldsymbol{x}_i^*,\boldsymbol{x}_j^*)$, and $\boldsymbol{K}(\boldsymbol{X}^*,\boldsymbol{X})\in\mathbb{R}^{\mathrm{k\,x\,n}}$ is the cross-covariance matrix with entries $K_{ij}=k(\boldsymbol{x}_i^*,\boldsymbol{x}_j)$.

2.2 Acquisition functions[1]

A popular acquisition function which works well in many scenarios is Expected Improvement (EI). Intuitively, if $\boldsymbol{f}^*=f(\boldsymbol{x}^*)=\max_{\boldsymbol{i=1,\cdots,n}}f(\boldsymbol{x}_i)$ is the best value so far observed, then a natural choice of quantity to maximize would be the difference between this and another potential observation $\max\{f(\boldsymbol{x})-f^*,0\}$, which is only non-zero if $f(\boldsymbol{x})>f^*$. While the true difference is unknown, its expectation under the Gaussian process posterior can be maximized instead, $\alpha_{\mathrm{EI}}=\mathrm{E}[\max\{f(\boldsymbol{x})-f^*,0\}]$. This quantity has a well-known closed form solution found via integration by parts [8]:

$$\alpha_{\mathrm{EI}}(\boldsymbol{x})=(\mu(\boldsymbol{x})-f^*)\Phi(\boldsymbol{z})+\sigma(\boldsymbol{x})\phi(\boldsymbol{z}) \qquad (5)$$

where $z=[\mu(\boldsymbol{x})-f^*]/\sigma(x)$, $\Phi(\cdot)$ is the CDF of the standard normal distribution, $\phi(\cdot)$ is the PDF of the standard normal distribution, and μ,σ are obtained from the predictive distribution of the surrogate of $f(\boldsymbol{x})$, namely, $\hat{f}(\boldsymbol{x})\sim N(\mu(\boldsymbol{x}),\sigma^2(\boldsymbol{x}))$. Expected Improvement has the p roperty that its value is high either where there is a good chance of finding a high function value or where the prediction uncertainty is high. A common strategy in the case of constrained optimization is to penalize inputs which are likely to violate the constraints [9]. If the m constraints are assumed to be statistically independent, then the probability a given $\boldsymbol{x}$ is feasible under all constraints, i.e., $\mathrm{P}[g_i(\boldsymbol{x})<0]$, $i=1,\cdots,m$, given $\hat{g}(\boldsymbol{x})\sim N(\mu(\boldsymbol{x}),\sigma^2(\boldsymbol{x}))$, can be expressed as:

$$\alpha_{\mathrm{PF}}(\boldsymbol{x})=\prod_{i=1}^{m}\Phi\left(\frac{0-\mu_i(\boldsymbol{x})}{\sigma_i(\boldsymbol{x})}\right),i=1,\dots,m \qquad (6)$$

[1] For visual clarity, dependence on ξ has been dropped from the notation in these subsections.

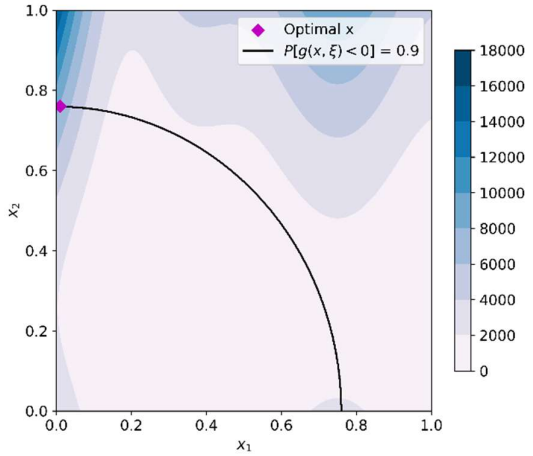

Figure 1: Branin-Hoo, contour plot of $E[f(\boldsymbol{x},\boldsymbol{\xi})]$.

2.3 Bayesian quadrature

In the chance constrained problem defined by Equation 1, it is not $f(\boldsymbol{x},\boldsymbol{\xi})$ that one seeks to maximize, as the above analysis assumes, but rather the expectation of f over the uncertain parameters, $a(\boldsymbol{x}) = \mathrm{E}[f(\boldsymbol{x},\boldsymbol{\xi})]$. It is possible to adapt the conventional Expected Improvement acquisition function accordingly. Our approach is similar to [10], in that we apply results from Bayesian quadrature [11] to integrate out the uncertain parameters from the objective and constraints in our chance constrained problem. In particular, we use the following:

$$\mathrm{E}[a(\boldsymbol{x})] = \int \mu(\boldsymbol{x},\boldsymbol{\xi})p(\boldsymbol{\xi})d\boldsymbol{\xi} := \mu_a(\boldsymbol{x}) \tag{7}$$

$$\mathrm{Cov}[a(\boldsymbol{x}), a(\boldsymbol{x}')] = \iint \Sigma\, p(\boldsymbol{\xi})p(\boldsymbol{\xi}')\, d\boldsymbol{\xi}d\boldsymbol{\xi}' \tag{8}$$

where $\Sigma = \Sigma(\boldsymbol{x},\boldsymbol{\xi},\boldsymbol{x}',\boldsymbol{\xi}')$ is the posterior predictive covariance of the Gaussian process model $\hat{f}$. Additionally, for the constraints, we use:

$$\mathrm{P}[g_i(\boldsymbol{x},\boldsymbol{\xi}) \le 0] = \int \Phi\left(\frac{0 - \mu_i(\boldsymbol{x})}{\sigma_i(\boldsymbol{x})}\right) p(\boldsymbol{\xi})d\boldsymbol{\xi} \tag{9}$$

Re-evaluating the acquisition functions in Section 2.2 given these results, the Expected Improvement relative to the current maximum $a^* = \max_{\boldsymbol{x}} \mathrm{E}[f(\boldsymbol{x},\boldsymbol{\xi})]$ under the Gaussian process posterior is given by:

$$\tilde{\alpha}_{\mathrm{EI}}(\boldsymbol{x}) = (\mu_a(\boldsymbol{x}) - a^*)\Phi(\boldsymbol{z}) + \sigma_a(\boldsymbol{x})\phi(\boldsymbol{z}) \tag{10}$$

where $z = [\mu_a(\boldsymbol{x}) - a^*]/\sigma_a(x)$, and $\sigma_a(\boldsymbol{x}) = \mathrm{Cov}[a(\boldsymbol{x}), a(\boldsymbol{x})] = \int \sigma^2(\boldsymbol{x},\boldsymbol{\xi})p(\boldsymbol{\xi})d\boldsymbol{\xi}$. The probability a given $\boldsymbol{x}$ is feasible is given by:

$$\tilde{\alpha}_{\mathrm{PF}}(\boldsymbol{x}) = \prod_{i=1}^{m} \mathrm{P}[g_i(\boldsymbol{x}) < 0], \qquad i = 1,\ldots,m \tag{11}$$

To find a new $\boldsymbol{x}$ point, one can use $\boldsymbol{x}_{\mathrm{new}} := \mathrm{argmax}_{\mathrm{x}}\, \tilde{\alpha}_{\mathrm{EI}}(\boldsymbol{x}) \times \tilde{\alpha}_{\mathrm{PF}}(\boldsymbol{x})$. This, however, leaves the uncertain parameter $\boldsymbol{\xi}$ undecided. Jurecka [12] suggests a simple approach; selecting $\boldsymbol{\xi}$ based on where both the Gaussian process model uncertainty is high, and where $\boldsymbol{\xi}$ is likely to occur, as defined by $p(\boldsymbol{\xi})$. If $\sigma^2(\boldsymbol{x},\boldsymbol{\xi})$ is an estimate for the squared error, weighting it by $p(\boldsymbol{\xi})$ leads to the acquisition function $\boldsymbol{\xi}_{\mathrm{new}} := \mathrm{argmax}_{\boldsymbol{\xi}}\, \sigma^2(\boldsymbol{x},\boldsymbol{\xi})p(\boldsymbol{\xi}) = \mathrm{argmax}_{\boldsymbol{\xi}}\, \alpha_{\mathrm{WSE}}(\boldsymbol{x},\boldsymbol{\xi})$.

3 ALGORITHM AND IMPLEMENTATION

3.1 Implementation

When optimizing the acquisition functions in algorithm 1, we use the Adam optimizer from PyTorch in batch mode [13], with Monte Carlo estimates of the integral expression defined by Equations 7, 8 and 9. Gradients are computed with PyTorch's automatic differentiation capabilities using the reparameterization trick [14] with a fixed set of base samples. Analytic expressions are possible for Equations 7, 8 and 9 when $p(\boldsymbol{\xi})$ is a normal density, but not for general $p(\boldsymbol{\xi})$. We note that many uncertainties which influence structures, such as imposed and dynamic loads, model uncertainties, and sometimes resistance parameters, are non-Gaussian [15]. Any suitable constrained optimization method can be applied to the constrained problem in the last step of Algorithm 1, outlined below. Since the test problems are relatively small, we conduct an exhaustive search to guarantee the optimal $\boldsymbol{x}^*$, as defined by the surrogate models, is found.

Algorithm 1 BayesOpt

1: Evaluate $f(\boldsymbol{x},\boldsymbol{\xi})$and $g_i(\boldsymbol{x},\boldsymbol{\xi})$ for the initial points $D = \{((\boldsymbol{x}_i,\boldsymbol{\xi}_i), f(\boldsymbol{x}_i,\boldsymbol{\xi}_i))\}_{i=1}^{n_0}$.
2: **for** $n = 1$ **to** N:
3: Solve $\boldsymbol{x}_{n+1} = \mathrm{argmax}_{\boldsymbol{x}}\, \tilde{\alpha}_{\mathrm{EI}}(\boldsymbol{x}) \times \tilde{\alpha}_{\mathrm{PF}}(\boldsymbol{x})$
4: Solve $\boldsymbol{\xi}_{n+1} = \mathrm{argmax}_{\boldsymbol{\xi}}\, \alpha_{\mathrm{WSE}}(\boldsymbol{x}_{n+1},\boldsymbol{\xi})$
5: Sample $f(\boldsymbol{x}_{n+1},\boldsymbol{\xi}_{n+1})$ and $g_i(\boldsymbol{x}_{n+1},\boldsymbol{\xi}_{n+1})$
6: Update the surrogates $\hat{f}$ and $\hat{g}_i$
7: **end for**
8: Return $\boldsymbol{x}^* = \mathrm{argmax}_{\boldsymbol{x}}\, \mathrm{E}[\hat{f}(\boldsymbol{x},\boldsymbol{\xi})]$ s.t. $\mathrm{P}[\hat{g}_i(\boldsymbol{x},\boldsymbol{\xi}) \le 0] \ge 1 - \varepsilon, \quad \forall\, i = 1,\ldots,m$

4 EXAMPLES

4.1 Branin-Hoo function

As a test problem we use the Branin-Hoo function described in [16] with the addition of a constraint function. The response function in this case is defined as the product $f(\boldsymbol{x},\boldsymbol{\xi}) = b(15x_1 - 5, 15\xi_1) \times b(15\xi_2 - 5, 15x_2)$, where b is given by:

$$b(u,v) = \left(v - \frac{5.1}{4\pi^2}u^2 + \frac{5}{\pi}u - 6\right)^2 + \left(10 - \frac{1}{8\pi}\right)\cos(u) + 10 \tag{12}$$

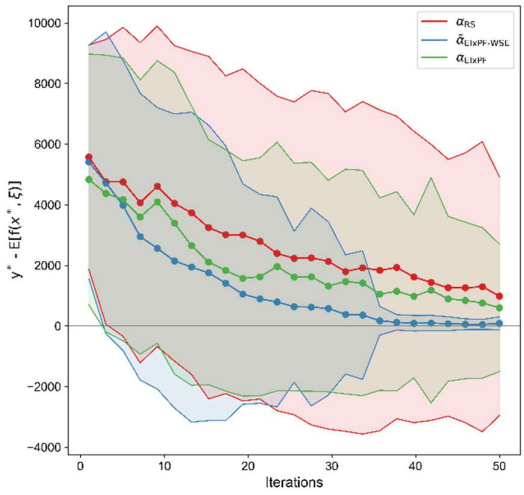

Figure 2: Branin-Hoo BayesOpt results.

The design variables are $\boldsymbol{x} \in [0,1]^2$, whilst the uncertain parameters $\xi \sim p(\boldsymbol{\xi})$ are drawn from the probability distribution described in Table 1. The support of the parameters ξ_1 is the set $\Xi_1 = \{0.25, 0.5, 0.75\}$ and likewise for ξ_2, its support is the set $\Xi_1 = \{0.2, 0.4, 0.6, 0.8\}$. The optimization problem for this example is given by the following two finite sums:

$$\mathrm{E}[f(\boldsymbol{x},\boldsymbol{\xi})] = \sum_{\xi \in \Xi_1 \times \Xi_2} f(\boldsymbol{x},\boldsymbol{\xi}) p(\boldsymbol{\xi}) \qquad (13)$$

$$\mathrm{P}[g_i(\boldsymbol{x},\boldsymbol{\xi}) \le 0] = \sum_{\xi \in \Xi_1 \times \Xi_2} 1_{\{g(\boldsymbol{x},\boldsymbol{\xi}) \le 0\}}\, p(\boldsymbol{\xi}) \qquad (14)$$

where $1_{\{\text{condition}\}}$ is an indicator function which is equal to 1 if condition = True, and 0 otherwise. A contour plot of the objective is shown in Figure 1. Figure 2 shows the distribution over algorithmic performance, in terms of mean line and 95% confidence bounds. The reliability level ε was set to 0.1. Two approaches, $\alpha_{\mathrm{EI}}(\boldsymbol{x}) \times \alpha_{\mathrm{RS}}(\boldsymbol{x})$ and $\tilde{\alpha}_{\mathrm{EI}}(\boldsymbol{x}) \times \tilde{\alpha}_{\mathrm{PF}}(\boldsymbol{x})$, have been investigated. For the former, only local information is used, whereas in the latter case, integration is performed over the stochastic parameters, as described in Section 2. The two algorithms are compared to random search, termed $\alpha_{\mathrm{RS}}(\boldsymbol{x})$. Figure 2 shows the error between the true $y^* = \max \mathrm{E}[f(\boldsymbol{x},\boldsymbol{\xi})]$ and $\mathrm{E}[f(\boldsymbol{x}^*,\boldsymbol{\xi})]$ for the $\boldsymbol{x}^* = \operatorname{argmax} \mathrm{E}[f(\boldsymbol{x},\boldsymbol{\xi})]$ proposed by each algorithm. The best performance was seen for the acquisition function $\tilde{\alpha}_{\mathrm{EI}}(\boldsymbol{x}) \times \tilde{\alpha}_{\mathrm{PF}}(\boldsymbol{x})$, which also had the tightest bounds. All three algorithms were run 40 times.

$\xi_1 \backslash \xi_2$	0.2	0.4	0.6	0.8
0.25	0.0375	0.0875	0.0875	0.0375
0.50	0.0750	0.1750	0.1750	0.0750
0.75	0.0375	0.0875	0.0875	0.0375

Table 1: Joint probability density $p(\boldsymbol{\xi})$.

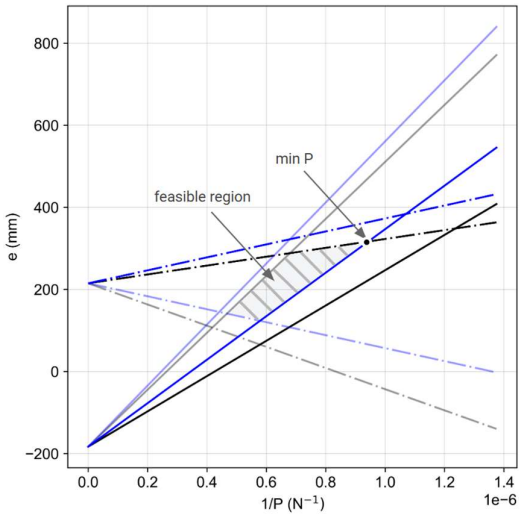

Figure 3: Magnel diagram.

4.2 *Prestressed concrete beam*

The BayesOpt algorithm is next applied to the design of a prestressed tie-beam. This example is taken from [18], who report on the various prestressing systems extant in Coventry Cathedral, UK. The tie-beam, which is also a pile cap, acts as part of an inverted portal frame to resist the lateral thrust generated at roof level by a shallow-arched shell (Figure 4). Several interesting uncertainties are present. The original designers assumed the line of thrust [of the loads from the roof onto the structure] to be at an angle 20° (see Figure 4), yet depending on the uniformity of the live load, the thrust line could more closely follow the profile of the roof. The moment taken by the beam is also unclear; the system is statically indeterminate, depending on the [unknown] support stiffnesses provided by the piles.

The prestress design is done in accordance with BS EN 1992-1-1:2004 and the UK National Annex [1]. Design checks are limited to the serviceability limit state. Tensile stresses should be avoided in the concrete, i.e., $\mathrm{f}_t = 0$. The concrete characteristic compressive strength f_{ck} is 30 MPa at service, and 20 MPa at transfer. To avoid cracking and excessive levels of creep, compressive stress in the concrete should be limited to $\mathrm{f}_{\mathrm{c}} = 0.6\,\mathrm{f}_{\mathrm{ck}}$. The steel tendons have a characteristic and design strength of $f_{\mathrm{pk}} = 1860$ MPa and $f_{\mathrm{p,max}} = 0.8 f_{\mathrm{pk}}$ respectively. The Young's modulus E of the concrete is 30 GPa. The density of concrete and steel is 24 kN/m^3 and 78.5 kN/m^3 respectively. The following relation describes the stress state at the top or bottom of the cross section:

$$f_c \ge \frac{P}{A} + \frac{Pe}{Z} - \frac{M}{Z} \ge f_t \qquad (15)$$

where P is the prestress force, A is the gross cross section area, e is the eccentricity from the neutral axis to the prestress force, Z is the gross section modulus of the

concrete, and M is the applied moment. Clearly $f_c \geq \sigma \geq f_t$ defines two inequalities, but if one considers that this equation applies to both the top and bottom of the section, i.e., Z is either Z_1 or Z_2, and accounting for a change in sign, then there are four inequalities.

$$-\frac{Z_1}{A}+\frac{f_c Z_1}{P}+\frac{M}{P} \leq e \leq -\frac{Z_1}{A}+\frac{f_t Z_1}{P}+\frac{M}{P} \qquad (16)$$

$$-\frac{Z_2}{A}+\frac{f_c Z_2}{P}+\frac{M}{P} \geq e \geq -\frac{Z_2}{A}+\frac{f_t Z_2}{P}+\frac{M}{P} \qquad (17)$$

If additionally, one considers both short- and long-term loading, there are eight inequalities. These eight inequalities, along with the practical spacing requirements, $e_{\min} \leq e \leq e_{\max}$, define the feasible space of combinations of prestress force P and eccentricity e which satisfy the serviceability limit state. These are typically plotted in $1/P - e$ space. Figure 3 shows such a plot, which is termed a Magnel diagram. Short- and long-term loading here refers to forces 1) at the transfer of prestress forces to the beam, where the prestress force and the self-weight must be considered, and 2) when the beam is under the influence of all of the applied load. Instantaneous and time dependent prestress losses are considered for case one and two respectively. Initial prestress losses due to elastic shortening, friction, and wedge draw-in of the anchorage are estimated as five percent of the initial prestress force, whilst time dependent losses due to creep and shrinkage are estimated as ten percent of the initial prestress force. These values lie within the typical range of losses encountered in design [17]. It is straightforward to linearize the equations governing the serviceability limit state, e.g.,$(f_c Z + M)R - e \geq Z/A$, where $F = 1/P$. For a given section, evaluating the serviceability can therefore be posed as a linear programming problem of the form:

$$\max_{\boldsymbol{z}\in\mathbb{R}^2} \mathbf{c}^{\mathrm{T}}\boldsymbol{z} \quad \boldsymbol{Qz} \leq \boldsymbol{b} \qquad (18)$$

where the minimum prestress (and therefore minimum cost) and associated eccentricity is the selected for. Here $\boldsymbol{c} = [1, 0]$, $\boldsymbol{z} = [F, e]$, and the inequalities $(f_i Z_i + M_i)R - e \leq Z_i/A$, $\forall\, i$ and bounds on e are collected in the matrix Q. If a feasible $\mathbf{z}$ can be found for a given section, then the associated set of inequalities are satisfied. The reliability problem (Equation 1) to be solved (which is negated to get minimum cost) is given by:

$$\mathrm{E}[f(\boldsymbol{x})] = C(\boldsymbol{x}) = V_c c_c + M_s c_s + A_f c_f \qquad (19)$$

$$\mathrm{P}[g(x,\xi) \leq 0] = \mathrm{P}\left[1_{\{f_c<\sigma \text{ or } \sigma<f_t\}} \leq 0\right] \qquad (20)$$

The design variables in this case are the breadth and height of the beam $\boldsymbol{x} \in [\mathrm{b}, \mathrm{h}]$, and the uncertain parameters are $\boldsymbol{\xi} = \left[\theta, k_A, k_{A,\theta}, k_B\right]$; the loading angle and the linear and rotational support stiffnesses. It is assumed the uncertainties are multivariate normal, $p(\boldsymbol{\xi}) \sim N\left(\boldsymbol{\mu}_{\xi}, \boldsymbol{\Sigma}_{\boldsymbol{\xi}}\right)$, with mean vector and covariance matrix:

$$\boldsymbol{\mu}_{\xi} = [27.5 \quad 0.015 \quad 1.5 \quad 0.015] \qquad (21)$$

$$\boldsymbol{\Sigma}_{\boldsymbol{\xi}} = \begin{bmatrix} \sqrt{15}/2 & 0 & 0 & 0 \\ 0 & 1 & 0.9 & 0.7 \\ 0 & 0.9 & 1 & 0.7 \\ 0 & 0.7 & 0.7 & 1 \end{bmatrix} \qquad (22)$$

The θ parameter is in the correct scale in the mean vector $\boldsymbol{\mu}_{\xi}$, however the stiffnesses k_A, k_B and $k_{A,\theta}$ should be scaled by 10^{10} to get the correct values in N/m or Nm/rad. The stiffness values are calibrated to produce at the extreme ends of the distribution a moment in the beam of between 2000 kNm and 20000 kNm, which represents either 10% or 90% of the total moment being taken by the beam. We assume the stiffnesses are strongly correlated; k_A and $k_{A,\theta}$ are assumed to vary with one another more strongly than either of them with k_B, to allow for local variations in the ground conditions. With reference to Equation 1, the reliability level ϵ was set to 0.1. The cost of the beam is calculated with the following cost coefficients for the concrete, prestressing tendons and formwork respectively: $c_c = 145\,£/\mathrm{m}^3, c_s = 9000\,£/$ tonne and $c_f = 36\,£/\mathrm{m}^2$. These quantities operate on the volume of concrete $V_c = b \times h \times L$, the plan area $A_f = b \times L$, and the mass of steel tendons required $M_s = \rho_s L \times P/f_{\mathrm{p,max}}$. The code for the stiffness matrix analysis and the prestressed design is available at: github.com/jamesalexwhiteley.

Figure 5 shows the BayesOpt results for the prestressed example. All three algorithms were run 50 times. Here again BayesOpt outperforms random search in terms of solution quality and robustness, with $\tilde{\alpha}_{\mathrm{EI}}(\boldsymbol{x}) \times \tilde{\alpha}_{\mathrm{PF}}(\boldsymbol{x})$ most closely targeting the true optimal design. Random search was effective in minimising the cost function, but not at ensuring the design was feasible under the constraint, hence producing designs smaller than the smallest feasible design, i.e., infeasible solutions.

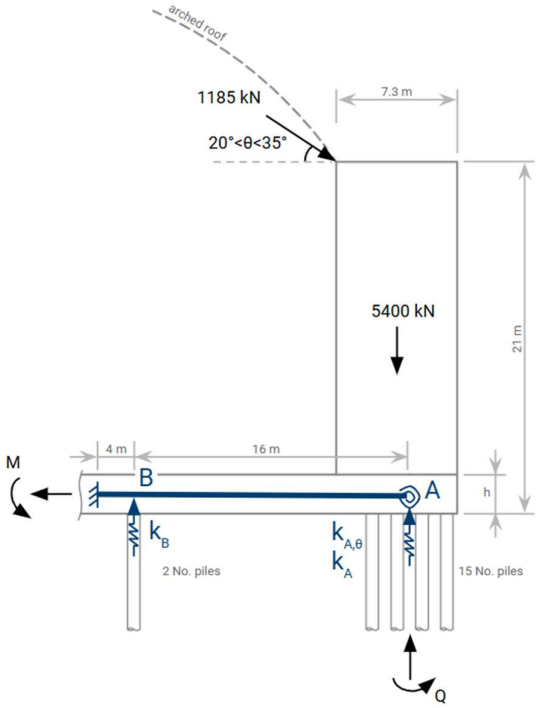

Figure 4: Prestressed tie-beam system (adapted from [18])

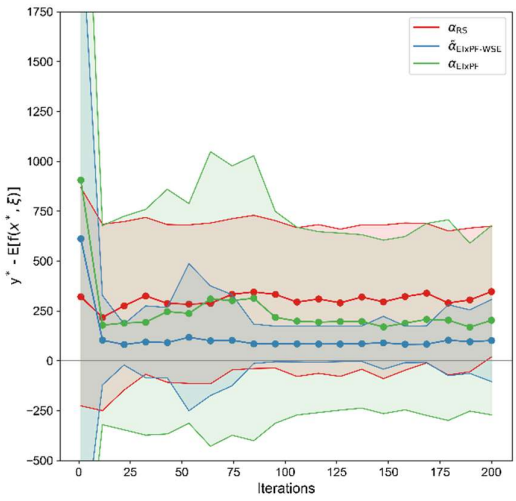

Figure 5: Prestressed beam BayesOpt results.

5 CONCLUSIONS

This paper presents a reliability-constrained Bayesian optimization framework for structural design under uncertainty. Whilst leveraging gradient-based, parallel batch optimization, this method offers a computationally efficient solution for managing uncertainties drawn from arbitrary probability distributions. Numerical results demonstrate the efficiency of this approach relative to generic surrogate modelling based on random search. Future research is suggested to focus on larger, real-world structural examples, using expensive finite-element analysis.

ACKNOWLEDGEMENTS

The authors would like to thank Laing O'Rourke Ltd for providing financial support and offering valuable research input throughout the course of the project. The authors gratefully acknowledge the EPSRC for funding this research through the EPSRC Centre for Doctoral Training in Future Infrastructure and Built Environment: Resilience in a Changing World, under grant number EP/S02302X/1.

REFERENCES

[1] BS EN 1990:2002+A1:2005 *Eurocode: Basis of structural design*. British Standards Institution (BSI), London, 2002.

[2] Ellingwood, B.R., *Development of a probability based load criterion for American National Standard A58: Building code requirements for minimum design loads in buildings and other structures,* US Department of Commerce, National Bureau of Standards, 1980.

[3] Campi M.C. and Garatti S., "A sampling-and-discarding approach to chance-constrained optimization: feasibility and optimality", *Journal of optimization theory and applications,* vol. 148, no. 2, pp. 257-280, 2011.

[4] Khachiyan L.G., "The problem of calculating the volume of a polyhedron is enumerably hard", *Russian Mathematical Surveys,* vol. 44, no. 3, 1989.

[5] Hilton H.H. and Morris Feigen M., "Minimum weight analysis based on structural reliability", *Journal of the Aerospace Sciences*, vol. 27, no. 9, pp. 641-652, 1960.

[6] Frazier, Peter I. "A tutorial on Bayesian optimization." *arXiv preprint,* arXiv:1807.02811, 2018.

[7] Williams, C.K.I. and Rasmussen C.E., *Gaussian Processes for Machine Learning*. MIT Press, Cambridge, Massachusetts, 2006.

[8] Jones D.R., Schonlau M. and Welch W.J., "Efficient global optimization of expensive black-box functions", *Journal of Global optimization*, vol. 13, 455-492, 1998.

[9] Schonlau M., Welch W.J. and Jones D.R., "Global versus local search in constrained optimization of computer models", *Lecture notes-monograph series*, pp. 11-25, 1998.

[10] Groot P., Birlutiu A. and Heskes T., "Bayesian Monte Carlo for the global optimization of expensive functions", *ECAI 2010*, IOS Press, pp. 249-254, 2010.

[11] O'Hagan. A., "Bayes–hermite quadrature", *Journal of statistical planning and inference*, vol. 29, no. 3, pp. 245-260, 1991.

[12] Jurecka F., *Robust Design Optimization Based on Metamodeling Techniques*, Ph.D. dissertation, Technische Universität München, Munich, Germany, 2007.

[13] Paszke, A., et al. "PyTorch: An imperative style, high-performance deep learning library", in *Advances in Neural Information Processing Systems*, vol. 32, 2019.

[14] Wilson, J.T., et al. "The reparameterization trick for acquisition functions," *arXiv preprint*, arXiv:1712.00424, 2017.

[15] JCSS, *Probabilistic Model Code, Part II—Load Models*, Technical Report, 2001.

[16] Williams, B.J., Santner T.J. and Notz W.I., "Sequential design of computer experiments to minimize integrated response functions," *Statistica Sinica*, vol. 10, no. 4, pp. 1133-1152, 2000.

[17] Utrilla, M.A. and Samartín, A., "Optimized design of the prestress in continuous bridge decks." *Computers & structures*, vol. 64, no. 1-4, pp. 719-728, 1997.

[18] Burgoyne C. and Mitchell O., "Prestressing in Coventry Cathedral," *Structures*, vol. 11, 2017.